3906 *Macromolecules* **2009**, *42*, 3906–3916
DOI: 10.1021/ma802741u

Macromolecules
ARTICLE

Mechanistic Aspects of Sterically Stabilized Controlled Radical Inverse Miniemulsion Polymerization

Genggeng Qi,[†] Bennett Eleazer,[†] Christopher W. Jones,*[,†] and F. Joseph Schork*[,‡]

[†]*School of Chemical & Biomolecular Engineering, Georgia Institute of Technology, 311 Ferst Dr., Atlanta, Georgia 30332, and* [‡]*Department of Chemical and Biomolecular Engineering, 2113 Building 090, University of Maryland, College Park, Maryland 20742*

Received December 9, 2008; Revised Manuscript Received April 8, 2009

ABSTRACT: The kinetics of RAFT inverse miniemulsion polymerization of acrylamide are presented. The polymerizations exhibit typical behavior of controlled polymerizations under conditions where the hydrolytic degradation of the RAFT agent is less favorable. The effects of different reaction parameters such as temperature, initiator concentration, pH of the aqueous phase, RAFT agent, and surfactant concentration on RAFT inverse miniemulsion polymerization are presented. The particle nucleation process in the inverse miniemulsion polymerizations is evaluated by the use of radical scavengers. The presence of RAFT agent was found to have a significant impact on the particle nucleation process. The fate of desorbed monomeric radicals in inverse miniemulsion polymerizations is evaluated by the comparison of the rates of propagation, re-entry, and termination. One of the potential reasons for the induction time observed in the RAFT inverse miniemulsion polymerizations is suggested to be associated with desorption of monomeric and oligomeric radicals from the particles to the continuous oil phase.

Introduction

Synthetic hydrophilic polymers are widely used in numerous applications and are a billon dollar market each year, including uses as flocculants,[1] drag reduction agents and drilling fluids,[2,3] paper making additives,[4] and in drug delivery.[5] However, there are various process challenges such as nonuniform mixing and heat transfer limitations that exist in large-scale industrial production of hydrophilic polymers.[6] To overcome these problems, free-radical inverse emulsion polymerization has been used for decades and has evolved into one of the main routes in industry to produce synthetic hydrophilic polymers. Understanding of the process originated from the pioneering work of John Vanderhoff and co-workers in 1962.[7] More recently, a free-radical inverse miniemulsion polymerization was developed.[8] Related to a conventional miniemulsion, which is an aqueous dispersion of relatively stable oil droplets within a size range of 50−500 nm prepared by strong shearing of a system containing oil, water, surfactants, and costabilizers,[9] an inverse miniemulsion disperses an aqueous monomer or solution in a continuous oil phase. Free-radical inverse miniemulsion polymerizations maintain typical properties of conventional miniemulsion polymerizations such as droplet nucleation and are superior to free-radical inverse emulsion polymerizations in process robustness, particle size uniformity, and colloidal stability.[8] However, free-radical inverse miniemulsion polymerization still offers only limited ability to precisely design the structures and properties of the polymer products. As a potential answer to this challenge, RAFT inverse miniemulsion polymerization was proposed by applying RAFT chemistry to inverse miniemulsion polymerizations.[10] RAFT polymerization, known for years as a powerful way to produce polymers with well-defined or special architectures, has attracted significant attention and has been applied in many different conventional emulsion and miniemulsion systems in the past decade.[11−27]

Inverse miniemulsion polymerization is a relatively new technique and has not been well studied. In addition, RAFT inverse miniemulsion polymerization is an even more recent technique. By combining RAFT polymerization with inverse miniemulsion, RAFT inverse miniemulsion polymerization can in principle take the advantages of both of these techniques and offer a convenient way to synthesize unique or well-defined structured water-soluble copolymers and colloids such as hydrophilic nanogels.

For inverse miniemulsions, the prevailing surfactants have to be steric, nonionic surfactants, or a combination of nonionic and ionic surfactants. In contrast, conventional miniemulsions are generally stabilized by solely ionic surfactants or a combination of ionic and steric, nonionic surfactants. When steric surfactants are used, the kinetic behavior of the inverse miniemulsion can be dramatically different from ionically stabilized conventional (o/w) miniemulsion polymerizations. Unfortunately, no effort has been devoted to investigate systematically the polymerization kinetics and mechanism of sterically stabilized inverse miniemulsion systems. Therefore, it is of significant importance from both industrial and academic perspectives to perform a detailed study on RAFT inverse miniemulsion polymerization.

Experimental Part

Materials. All chemicals were purchased from Aldrich unless otherwise stated. Acrylamide (Am, >99.5%) was recrystallized from chloroform (>99.8%). Acrylic acid (AAc, >99.0%) was distilled under reduced pressure prior to use. Sodium sulfate (>99.0%), tetrahydrofuran (>99.9%), 2,2-diphenyl-1-picrylhydrazyl (DPPH, ∼95%), azoisobutyronitrile (AIBN, 98%), sodium hydroxide (50 wt % in H_2O), and cyclohexane (>99.5%) were used without further purification. The water-soluble initiator, 2,2′-azobis[2-(2-imidazolin-2-yl)propane] dihydrochloride (VA-044, >98%, Figure 1), was purchased from Wako and used as received. Deionized water

*Corresponding authors. E-mail: cjones@chbe.gatech.edu (C.W.J.); fjschork@umd.edu (F.J.S.).

 Published on Web 04/30/2009

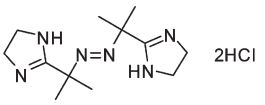

2,2'-Azobis[2-(2-imidazolin-2-yl) propane] dihydrochloride (VA-044)

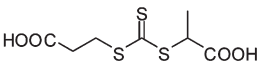

2-(2-carboxyethyl-sulfanylthiocarbonylsulfanyl) propionic acid (CTA)

Figure 1. Chemical structure of the initiator and the RAFT agent used in this study.

Table 1. Typical Recipe for Free-Radical and RAFT Inverse Miniemulsion Polymerization of Acrylamide

	component			
	free-radical mini	RAFT mini	mass (g)	notes
	cyclohexane	cyclohexane	40	
surfactant	B246	B246	0.60	1.5 wt % based on oil
	H_2O	H_2O	7.5	
monomer	acrylamide	acrylamide	2.5	3.62 M
initiator	VA-044	VA-044	0.028	[AM]:[initiator] = 400:1
costabilizer	Na_2SO_4	Na_2SO_4	0.10	1 wt % of aqueous phase
RAFT		CTA	0.089	[AM]:[CTA] = 100:1

was generated with a U.S. Filter Systems Deionizer and was used without further purification. B246SF, the steric surfactant, was kindly supplied by Uniqema. Unfortunately, very limited information about its chemical structure is available from open sources. It was reported this nonionic surfactant is a ABA triblock copolymer with a number-average molar weight around 3500 g mol^{-1}, where block A is poly(12-hydroxystearic acid) and block B is a poly(ethylene oxide).[28]

RAFT Agent Synthesis. The RAFT agent, 2-(2-carboxyethylsulfanylthiocarbonylsulfanyl)propionic acid (CTA, Figure 1), was synthesized according to literature procedures,[29] using the following materials without further purification: 3-mercaptopropionic acid (99%) and acetone (>99.5%) from Alfa Aesar. Two macro-RAFT agents were synthesized from the above RAFT agent by the solution polymerization of acrylamide in water at 45 °C. As an example, in a 50 mL flask 1.59 g of AM, 0.81 g of CTA, and 0.010 g of VA-044 were dissolved by 10 mL of water. The mixture was purged with N_2 and heated to 45 °C. After polymerization for 4 h, the reactant mixture was slowly poured into 100 mL of chilled methanol under rigorous stirring. The macro-RAFT agent was separated by centrifuge at 0 °C and then dried in vacuum oven at 40 °C for 48 h. For macro-RAFT1, M_n = 623, PDI = 1.43 and for macro-RAFT2, M_n = 2305, PDI = 1.25, as measured by GPC.

Inverse Miniemulsion Polymerization. The RAFT inverse miniemulsions were prepared according to the following procedure. As an example, 0.6 g of B246SF was dissolved in 40 g of cyclohexane to prepare the continuous phase of the inverse miniemulsion. The dispersed phase was prepared separately by adding 2.5 g of acrylamide, 0.028 g of VA-044, 0.089 g of RAFT agent, and 0.10 g of Na_2SO_4 (costabilizer) to 7.5 g of water and degassed under reduced pressure for 5 min. The inverse emulsion was prepared by dropwise addition of the dispersed phase to the B246SF cyclohexane solution and stirred under nitrogen at 10 °C for 40 min. The coarse inverse emulsion was then sonicated with a Fischer Model 30 sonic dismembrator operated at 70% power output for ~5 min under nitrogen. The free-radical inverse miniemulsions were prepared in a similar manner as RAFT inverse miniemulsions except that no RAFT agent was added to the aqueous phase. A typical recipe for the inverse miniemulsions is shown in Table 1.

The RAFT inverse miniemulsion prepared above was transferred into a 100 mL flask with a magnetic stirring bar. Inverse miniemulsion polymerizations were carried out in an oil bath preheated to 60 °C unless otherwise specified. The stirring rate was kept around 300 rpm. Samples were taken during the polymerizations to provide kinetic data. For RAFT inverse miniemulsion polymerizations, the samples were separated into two parts: one part was diluted with water-saturated cyclohexane for particle size determination, and another was quenched with drops of 1 wt % hydroquinone acetone solution for conversion measurements. For free-radical inverse miniemulsion polymerizations, the samples were also divided into two parts: a small portion of the samples was used for particle size analysis, and the other was quickly precipitated in excess chilled acetone containing 0.1 wt % hydroquinone for measurements of conversion by gravimetry.

Characterization. The molecular weight of the poly(acrylamide) samples was measured by aqueous gel permeation chromatography (GPC) at 30 °C. The GPC system was comprised of a Shimadzu LC-20AD pump, a Shimadzu RID-10A RI detector, a Shimadzu SPD-20A UV detector, a Shimadzu CTO-20A column oven, and Viscotek TSK Viscogel PWXL Guard, G3000 and G6000 columns mounted in series. The mobile phase was 0.05 M Na_2SO_4, and the flow rate was maintained at 0.5 mL/min. A poly(ethylene oxide) narrow standard kit from Aldrich was used to calibrate the GPC by the universal calibration method. The Mark−Houwink parameters of poly(acrylamide) in 0.05 M Na_2SO_4 are α = 0.66 and K = 0.000 373; for poly(ethylene oxide), α = 0.693 and K = 0.000 365.[30] The GPC samples were prepared according to the following procedure: latex aliquots of 1 mL were removed during the polymerization, quenched with drops of 0.1 wt % hydroquinone acetone solution in an ice bath, followed by vacuum drying at 30 °C to remove the volatile organics and water. The dried samples were redispersed in 10 mL of 0.05 M Na_2SO_4 aqueous solution, stored in the dark for 24 h at 5 °C, and then filtered with a 0.2 μm nylon filter. Shimadzu EZ-start V7.3 software was used for the analysis of molecular weight and polydispersity of poly(acrylamide).

For RAFT inverse miniemulsion polymerizations, the conversions of the monomer were determined with GPC by comparing the area of the RI signal corresponding to the monomer and the polymer.[31] For free-radical inverse miniemulsion polymerization, the conversions were measured gravimetrically: 3 mL miniemulsion aliquots were taken at certain intervals during the polymerizations and precipitated with chilled acetone containing 0.1 wt % hydroquinone. The polymers were washed with copious chilled acetone and separated by a centrifuge. The polymer samples were then vacuum-dried at 70 °C for 48 h, and the conversion was measured gravimetrically. Low molecular weight poly(acrylamide) has a finite solubility in the precipitating solvent, which lead to significant errors using the gravimetric method for the RAFT polymerizations at low conversions, and this is why the GPC method was used for conversion measurement for RAFT polymerizations.

Latex particle sizes and polydispersities were analyzed using quasi-elastic light scattering (QELS, Protein Solutions DynaPro with DynaPro DCS v 5.26 software). The inverse latexes were diluted with filtered water-saturated cyclohexane to a volume fraction of 0.5% of the dispersed phase. The total particle number N_p was estimated with the following equation:

$$N_p = \frac{m}{\frac{4}{3}\pi \bar{r}^3 \rho}$$

where m is the concentration of the dispersed phase (including both water and the monomer) in g/L cyclohexane, $\bar{r}$ is the average radius of particles, and ρ is the density of the particles, which can be estimated by assuming the dispersed phase as an idea solution:

$$\rho = \frac{1}{\frac{1-w}{\rho_{water}} + \frac{w(1-x)}{\rho_{acrylamide}} + \frac{wx}{\rho_{polyacrylamide}}}$$

where w is the initial weight percentage of acrylamide in the dispersed phase, x is the conversion of acrylamide, and ρ_{water}, $\rho_{acrylamide}$, and $\rho_{polyacrylamide}$ are density of water, 1.00 g/cm^3, acrylamide, 1.13 g/cm^3, and polyacrylamide, 1.30 g/cm^3, respectively.

The stability of the inverse miniemulsions was evaluated by their shelf lives, which were determined to be the time before significant phase separation of the stored inverse miniemulsions was visually observed at room temperature.

The solubility of RAFT agent in the oil phase was measured with a Hewlett-Packard 8453 UV/vis spectrophotometer. Because the low solubility of RAFT agent in cyclohexane, RAFT agent was diluted in a cyclohexane tetrahydrofuran solution (v:v = 10:1) to different concentrations for calibration. An inverse emulsion was prepared according to the typical recipe of RAFT inverse miniemulsion in Table 1, except that no initiator was added in the aqueous phase. The emulsion was mixed overnight and then centrifuged. After filtration with a 0.2 μm filter, the supernatant was mixed with tetrahydrofuran in a volume ratio of 10:1 for the solubility measurement, which was made by comparing its absorption at 315 nm with the calibration standards.

Results and Discussion

Effect of Reaction Parameters. Experiments 1−10, as shown in Table 2, explored the effects of different reaction parameters on the kinetics of RAFT inverse miniemulsion polymerization. The effect of temperature on the polymerization is shown in Figure 2. The rate of polymerization increased at a higher temperature. A longer induction time was observed at the lower temperature of 52 °C. This is likely due to both a lower propagation rate constant and a smaller population of free radicals generated from initiator at lower temperatures.

Figure 3 shows the conversion−time curves at two different initiator concentrations. The polymerization rate increased with an increasing amount of initiator since more radicals can be generated. The amount of initiator had no effect on the final particle size, as shown in Table 2. All the particle radii in Exp4 and Exp5 were close to 100 nm throughout the polymerization.

The pH of the dispersed phase is one of the key parameters that can affect the kinetics of RAFT inverse miniemulsion polymerizations. The aqueous solutions of Exp4, Exp6, and Exp7 were adjusted with NaOH to a pH of 4, 7, and 10, respectively, before the preparation of the inverse miniemulsions, with all other recipe variables kept constant, as shown in Table 2. Figure 4 shows the evolution of monomer conversion with reaction time at the different pHs. When the aqueous solution was weakly acidic or neutral, the conversion−time curves overlaid well. At pH = 10, the polymerization rate was trivially affected by the pH before the conversion reached around 50%, at which point a higher polymerization rate was observed compared to the lower pH runs.

The relationship between molecular weight and conversion is shown in Figure 5. There is a deviation of the experimental M_n from the theoretical prediction that may be caused by the GPC calibration method.[32] The M_n generally increased with conversion in a linear manner, except that slightly higher M_n was found at high conversions in Exp7 (pH = 10). The PDI in Exp7, however, showed a significant difference from Exp4 and Exp6 (Figure 5). The PDI at pH = 10 remained below 1.5 before 50% conversion, although it was slightly larger than in the experiments at pH = 4 and pH = 7, followed by a sharp increase of PDI up to 3.5.

The evolution of the RI curve from the GPC compared with the UV curve monitored at 311 nm is shown in Figure 6 for the experiments at different pH values. The UV curve

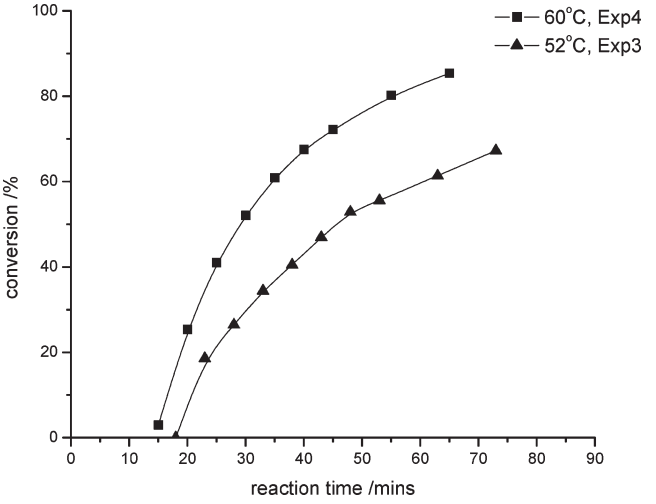

Figure 2. RAFT inverse miniemulsion polymerization of acrylamide at different reaction temperatures.

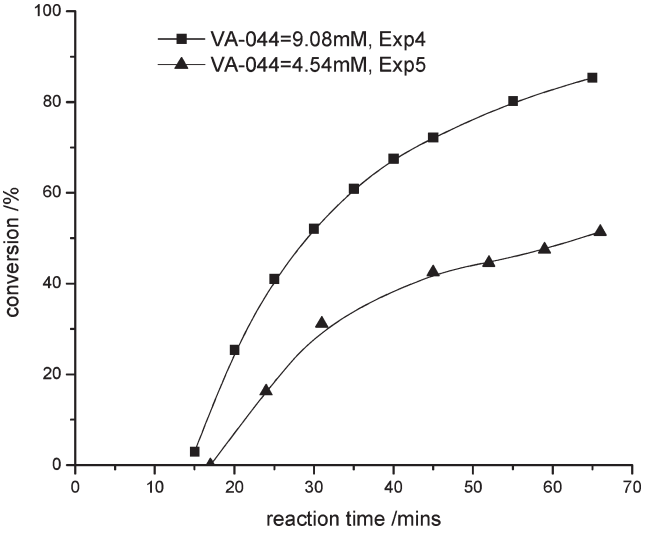

Figure 3. RAFT inverse miniemulsion polymerization of acrylamide at 60 °C with different amounts of initiator.

Table 2. Recipes for RAFT Inverse Miniemulsion Polymerization of Acrylamide

Exp	polymerization	monomer (M)	initiator (mM)	CTA (mM)	CTA/monomer	monomer/CTA	B246 (wt %)	temp (°C)	pH	$\bar{r}_w$ (nm)
1	RAFT solution	3.62	9.08	36.2	3.99	100		60	4	
2	free-radical mini	3.62	9.08				1.5	60	4	98
3	RAFT mini	3.62	9.08	36.2	3.99	100	1.5	52	4	102
4	RAFT mini	3.62	9.08	36.2	3.99	100	1.5	60	4	105
5	RAFT mini	3.62	4.54	36.2	7.98	100	1.5	60	4	103
6	RAFT mini	3.62	9.08	36.2	3.99	100	1.5	60	7	107
7	RAFT mini	3.62	9.08	36.2	3.99	100	1.5	60	10	99
8	RAFT mini	3.62	9.08	57.9	6.37	63	1.5	60	4	108
9	RAFT mini	3.62	9.08	36.2	3.99	100	1.0	60	4	112
10	RAFT mini	3.62	9.08	36.2	3.99	100	2.5	60	4	103
11[a]	RAFT mini	3.62	9.08	36.2	3.99	100	1.5	60	4	110
12[b]	RAFT mini	3.62	9.08	36.2	3.99	100	1.5	60	4	114

[a] Macro-RAFT1 was used as CTA. [b] Macro-RAFT2 was used as CTA.

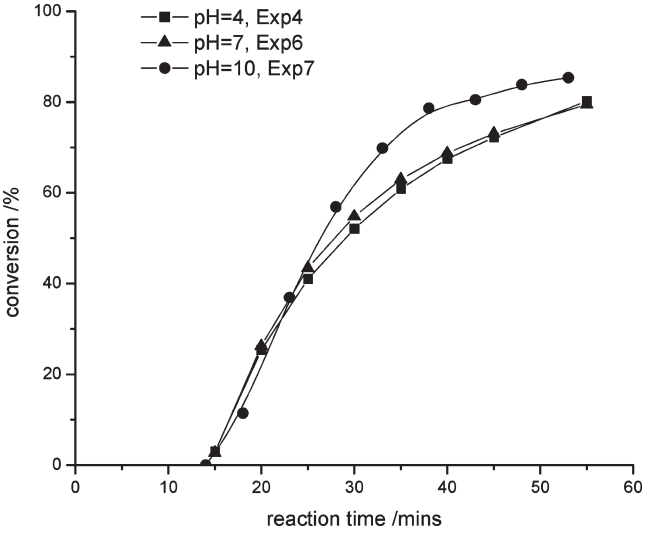

Figure 4. RAFT inverse miniemulsion polymerization of acrylamide at 60 °C at different pH values.

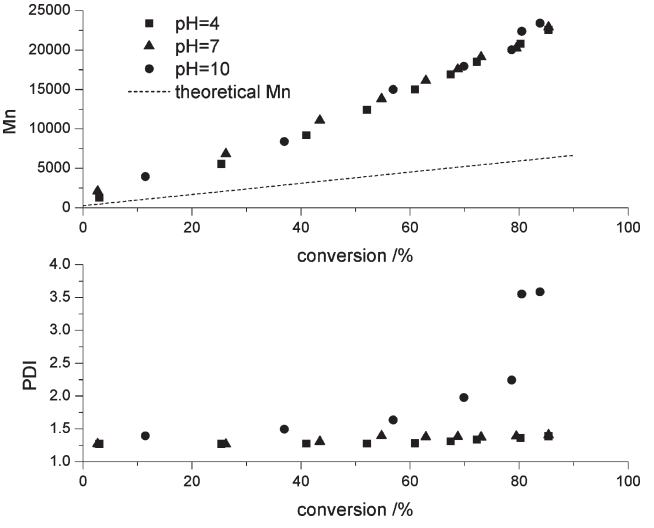

Figure 5. Relationship between M_n, PDI, and conversion in RAFT inverse miniemulsion polymerization of acrylamide at 60 °C at different pH values.

corresponds to the signal from the C=S bond in the RAFT agent, giving a measure of the polymer chains that contain a RAFT functional group (potentially "living chains"), while the RI curve accounts for all the polymer species in the system.[33] Therefore, the content of living chains among all the polymer chains can be estimated by the degree of overlap

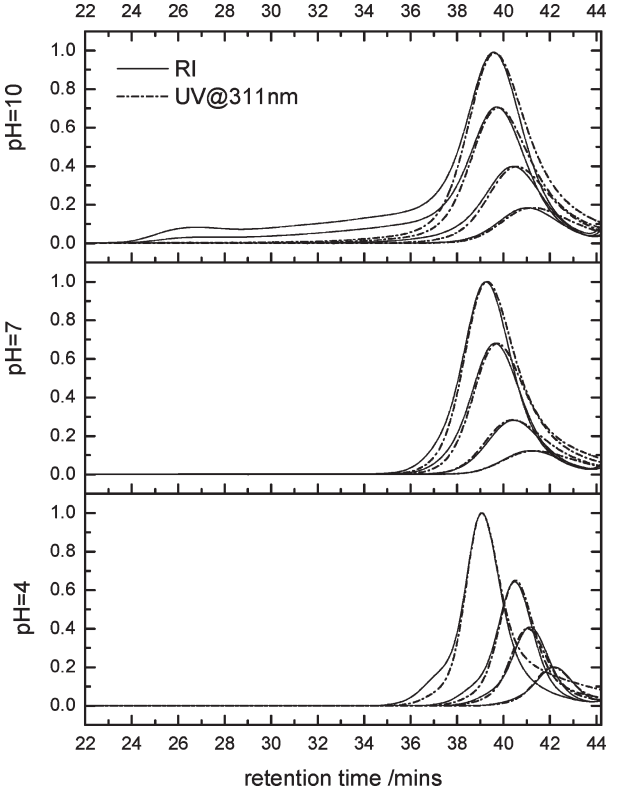

Figure 6. GPC chromatograms (RI and UV traces at 311 nm) showing the evolution of the RAFT inverse miniemulsion polymerization of acrylamide at different pH values.

of the two curves. In Exp4 and Exp6, the overall RI signals had a very good overlay with the UV curves throughout the RAFT inverse miniemulsion polymerizations, in spite of the small shoulder in the RI curve at shorter retention times. This is likely caused by termination between the propagating radicals or propagating radicals and RAFT intermediates. However, significant deviation of RI and UV curves was observed in Exp7 (pH = 10) with increasing conversion. The RI curve skewed to high molecular weight, and this resulted in a much broader PDI. The reduced control at higher conversions at pH = 10 may result from the hydrolysis of the RAFT agent, among other factors, a well-known issue in aqueous RAFT polymerizations.[34]

Different groups have reported very similar behavior in RAFT solution polymerizations as a result of RAFT agent hydrolysis.[34−37] Although trithiocarbonates were found to be a more preferable RAFT agents than dithioesters for the polymerization of acrylamide and are thought to be fairly stable when the pH is lower than 7, they can be easily

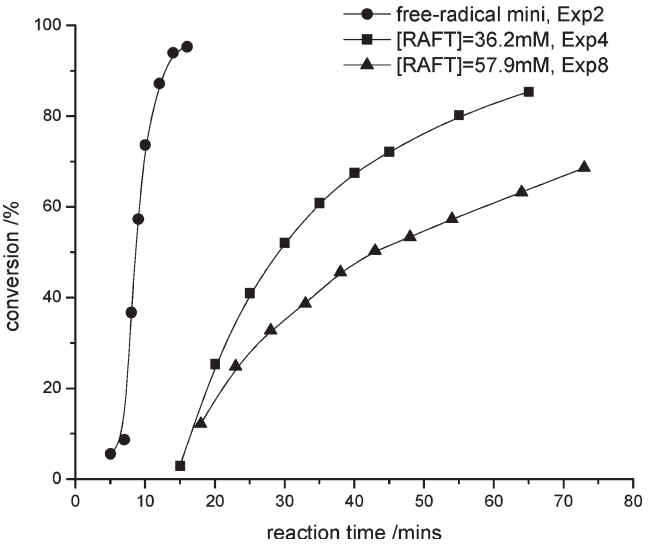

Figure 7. RAFT inverse miniemulsion polymerization of acrylamide at 60 °C with different RAFT agent concentrations.

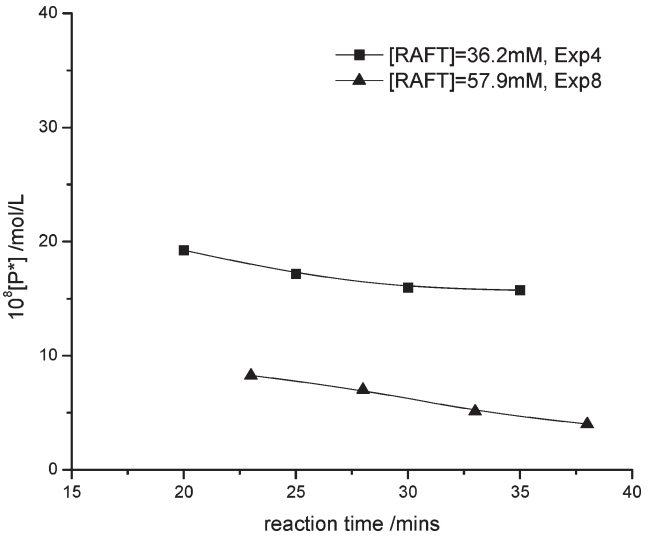

Figure 8. Apparent total propagating radical concentration in RAFT inverse miniemulsion polymerization of acrylamide with varying RAFT agent concentration.

hydrolyzed in basic solution.[35,38] The good overlap between the RI and UV signals in Exp4 and Exp6 and the significant increase in the high molecular weight shoulder with prolonged reaction time in Exp7 (pH = 10) suggests the loss of control in Exp7 is likely attributable to hydrolysis of the RAFT agent. The poor overlap of the GPC curves in Exp7 is also consistent with the significantly broader PDI of Exp7.

The effect of RAFT agent concentration on the polymerization was studied by the comparison of Exp4 and Exp8. With an increase of RAFT concentration from 36.2 mM (Exp4) to 57.9 mM (Exp8), a significant rate retardation was observed (Figure 7). More retardation is usually observed in conventional o/w miniemulsion polymerizations in the presence of a larger amount of RAFT agent. A variety of possible causes have been proposed in the literature for this observation, and these may be applicable to the RAFT inverse miniemulsion polymerization studied here. First, RAFT-induced radical exit and oligomeric radical desorption from the polymer particles may lead to retardation.[39,40] More shorter chain radicals will be produced at a higher concentration of RAFT agent, and these are more likely to desorb from the particles and lead to a lower average number of propagating radicals in each particle. From the conversion−time curves of Exp4 and Exp8, the apparent total propagating radical concentration [P•] during the polymerizations of Exp4 and Exp8 can be roughly estimated by the following equation:[41]

$$[\mathrm{P}^\bullet] = \frac{\mathrm{d}[-\ln(1-x)]}{k_\mathrm{p}\,\mathrm{d}t}$$

where x is the conversion of monomer. The propagating coefficient of acrylamide at 60 °C was reported to be $k_\mathrm{p} = 2.58 \times 10^6$ L/(mol min^{-1}),[42] which agrees well with a more recent report based on pulsed laser polymerization method.[43] To avoid the potential influences of the gel effect and chain length dependence of k_p in the polymerizations, only the conversion data between 25% and 55% were used for analysis. As shown in Figure 8, the apparent total propagating radical concentration [P•] in Exp4 and Exp8 appeared to decrease slightly with reaction time but still remained on the same order of 10^{-8} mol/L. When a higher concentration of RAFT agent was used, a lower [P•] resulted in the system.

Another reason for the rate retardation may be associated with the compartmentalization of RAFT miniemulsion polymerization.[44] If the RAFT miniemulsion polymerization is a zero-one system, the intermediate and propagating radicals are segregated in separate particles. There is a quantitative relationship between the average number of radicals per particle in a RAFT miniemulsion polymerization, $\bar{n}_\mathrm{RAFT}$, compared to a free-radical miniemulsion polymerization $\bar{n}_\mathrm{free\text{-}radical}$: $1/\bar{n}_\mathrm{RAFT} = 1/\bar{n}_\mathrm{free\text{-}radical} + 2K_\mathrm{eq}[\mathrm{RAFT}]_0$, where K_eq is the chain transfer constant for the main equilibrium of RAFT process.[44] A larger RAFT concentration will result in a lower average number of radicals per particle and thus a more pronounced retardation. It should be noted that it is difficult to tell conclusively based on the data here whether radical desorption, compartmentalization, or some combination of these factors caused the lower apparent total propagating radical concentration at the higher RAFT concentration.

It is helpful to compare the change of average number of radicals per particle with the concentration of RAFT to shed some light on the above compartmentalization assumption. The average number of radicals per particle, $\bar{n}$, can be calculated with the following equation:

$$\bar{n} = \frac{M_0 N_\mathrm{A}}{k_\mathrm{p}[\mathrm{M}]_\mathrm{p} N_\mathrm{p}} \frac{\mathrm{d}x}{\mathrm{d}t}$$

where M_0 is the initial total monomer amount (mol) in the system, N_A is Avogadro's constant, and k_p is the propagation coefficient of the monomer (L/(mol min)). N_p is the total particle number, and x is the conversion of the monomer. Note that a large amount of water was used in the inverse miniemulsion to dissolve the monomer. Both water and Na_2SO_4 can act as osmotic agents and significantly limit the mass transfer of the monomer between phases.[45] Therefore, $[\mathrm{M}]_\mathrm{p}$, the monomer concentration in the latex particles (mol/L), can be estimated simply from the monomer conversion x: $[\mathrm{M}]_\mathrm{p} = [\mathrm{M}]_0(1-x)$, in which $[\mathrm{M}]_0$ is the initial monomer concentration in the dispersed phase. From Figure 9, the $\bar{n}$ values in both Exp4 and Exp8 were far below 0.5. The theoretical prediction of the average number of radicals per particle for Exp4 and Exp8 is in good agreement with the experimental results.

Figure 10 shows the relationship between M_n and the conversion in Exp4 and Exp8. The M_n increased linearly

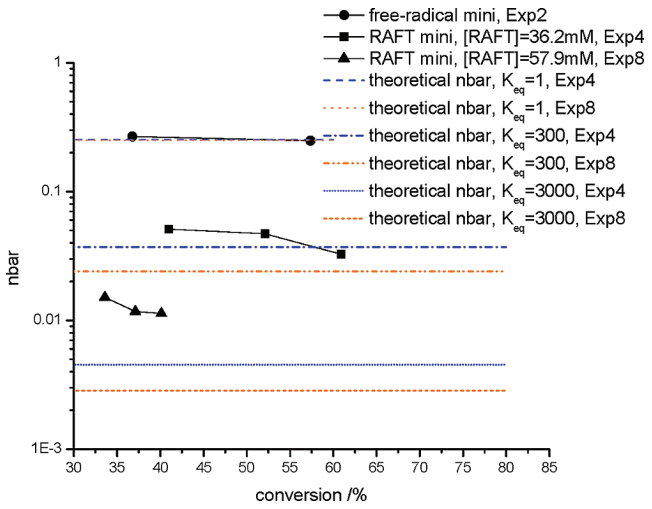

Figure 9. Evolution of the average number of propagating radicals per particle as a function of conversion in RAFT inverse miniemulsion polymerizations at 60 °C. $\bar{n}_{\text{free-radical}} = 0.26$. The chain transfer constant of the main step of RAFT process K_{eq} is set as an adjustable parameter.

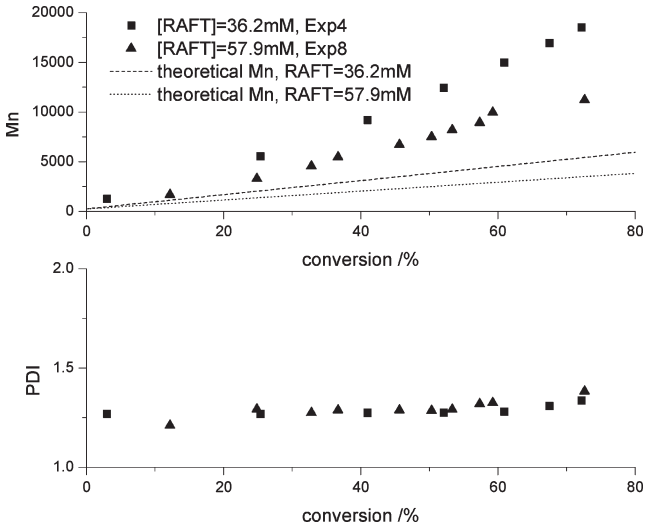

Figure 10. Relationship between M_n, PDI, and conversion in RAFT inverse miniemulsion polymerizations of acrylamide at 60 °C with different RAFT concentrations.

with the conversion and, as expected, decreased with an increase in RAFT agent concentration. In both cases, the PDIs remained below 1.3 until the end of the polymerizations.

In the previous study of free-radical inverse emulsion polymerizations, the correlation between the polymerization rates and the surfactant concentration was found to be more complicated compared to normal o/w systems. For example, the reaction temperature and the continuous oil solvent can affect micelle formation and the interactions between the surfactants and droplets in inverse emulsion polymerizations. Additionally, the nature of the initiator affects the primary radical location, i.e., in the continuous phase vs in the monomer droplets. It was found that when oil soluble initiators were used, polymerizations carried out at higher temperatures and using aromatic solvents as the continuous phase tended to have positive reaction orders with respect to surfactant concentration, while negative reaction orders could occur when using aliphatic media at low reaction temperatures and with high surfactant levels.[46−48] If water-soluble initiators were used, the polymerization kinetics

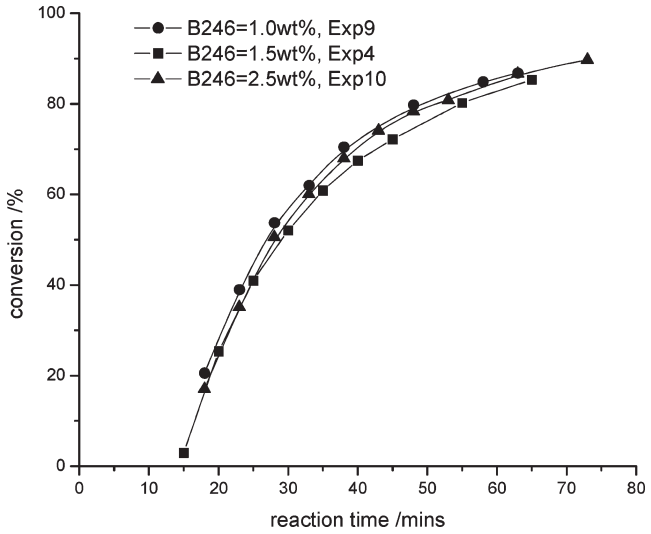

Figure 11. RAFT inverse miniemulsion polymerization of acrylamide at 60 °C with different surfactant concentrations.

of inverse emulsion polymerizations were similar to the solution or bulk polymerization controls, which is significantly different from that of o/w emulsion polymerizations.[46−48] To the best of our knowledge, the effect of surfactant concentration on the kinetics of RAFT inverse miniemulsion polymerization has not been studied to date. Moreover, steric surfactants are generally used in inverse miniemulsion polymerizations, and these can dramatically affect the reaction kinetics because of the barrier effects of the surfactant[22,23] as well as potential chain transfer reactions to the surfactant molecules.[47,49] Therefore, it is of significant importance to investigate the effects of the surfactant concentration on the polymerization kinetics of inverse miniemulsion polymerization here. To this end, in Exp4, Exp9, and Exp10, the amount of surfactant was increased from 1 to 2.5 wt % based on the oil phase. As shown in Figure 11, there seems to be no change in the polymerization rate at the different surfactant concentrations in our study. The average particle radius remained almost constant at ~105 nm under different surfactant concentration levels, as shown in Table 2. These results agree with a previous study of inverse microsuspension polymerization of acrylamide where the polymerization rate, the average particle diameter, and the radical capture efficiency were essentially independent of the emulsifier,[47] indicative of the purely physical role of B246 and the dominant droplet nucleation feature in our inverse miniemulsion polymerizations.

Particle Nucleation Difference in Free-Radical and RAFT Inverse Miniemulsion Polymerization. For miniemulsion polymerizations, initiators are usually dissolved in the continuous phase, and the polymerization mechanism has been well studied.[50−52] When an initiator is used in the dispersed phase of a miniemulsion, the efficiency of the initiator is usually significantly lower than that of solution and bulk controls although the kinetic behavior of such miniemulsion polymerizations is very similar to that with initiators in the continuous phase.[53] To clarify the reason for the low initiation efficiency, two primary theories have been proposed and have been subject to vigorous debate over the past decade. The focus has been on the dominant radical location, resulting in particle nucleation. Nomura et al. claimed that the fraction of initiator partitioned in the continuous phase plays a decisive role in particle nucleation since the radicals produced in a pairwise manner in the particles may result

in geminate termination instantaneously.[54] Asua et al., however, suggested that pairwise radicals are generated by initiator decomposition within the particles and particles are nucleated by those single radicals left inside the droplets by desorption at least one of the pairwise radicals into the continuous phase.[55] Both of the theories have been supported by varied and in many cases conflicting experimental evidence and theoretical simulations of conventional oil-in-water miniemulsion polymerizations.[56−58]

The initiator used in this study, VA-044, was dissolved in the dispersed phase since our previous study showed that using a water-soluble initiator had some advantages over an oil-soluble initiator in achieving controlled polymerization by limiting homogeneous nucleation.[10] Unfortunately, the particle nucleation process in RAFT inverse miniemulsion polymerizations have not been explored before; therefore, we seek to explore this issue since identification of the main radical source for particle nucleation is very important to understand the mechanism of RAFT inverse miniemulsion polymerization. A set of experiments (Exp13−Exp17) was used to explore this issue.

DPPH, a water-insoluble radical scavenger widely used for antioxidant assays, was added to the cyclohexane to trap the active radicals in the continuous phase of the inverse miniemulsions. The effects of DPPH on the kinetics of RAFT inverse miniemulsion polymerizations were quite different from the free-radical inverse miniemulsion polymerizations. For the RAFT inverse miniemulsion polymerizations Exp13, Exp14, and Exp15, DPPH was added to the continuous phase at a conversion of 24%, 42%, and 56%, respectively. As shown in Figure 12, the conversion−time curves generally were all identical, up to the point of DPPH addition, when a plateau occurred. The duration of the plateau period was shorter in Exp13, compared with Exp14 and Exp15, where DPPH was added at a higher conversion and where the plateau periods were similar. These data suggest that once the added DPPH was consumed, the polymerization continued again and the conversion increased with reaction time. These results indicate that radicals in the continuous phase may be the dominant source to initiate the controlled polymerizations.

Since there was a concern that a small fraction of DPPH might diffuse into the particle and terminate the polymerizations, Exp16 used acrylic acid instead of DPPH to assess the main radical location. It should be pointed out that acrylic acid is a more preferable monomer here compared to hydrophobic monomers such as styrene, since it allows any potential copolymerization to be assessed by GPC and, at the same time, rules out the formation of amphiphilic copolymers of acrylamide that may affect the polymerization mechanism. In Exp16, 0.72 g of acrylic acid was added to the oil phase (∼195 mM) when the conversion of the RAFT inverse miniemulsion polymerization was at ∼39%. Samples (∼1 mL) of the inverse miniemulsion were taken before and after the addition of acrylic acid for particle size and shelf life measurement. No change of particle size was observed from QELS, and both of the inverse miniemulsions had a shelf life > 7 days. These results suggest the addition of acrylic acid had no significant effect on the stability of inverse miniemulsion. In Exp16, the aqueous phase had a pH = 4, and the volume ratio of the aqueous phase to cyclohexane was around 0.19. Therefore, it is estimated that most of acrylic acid was partitioned into the cyclohexane phase.[8] When the conversion was ∼39%, most of the radicals are polymeric in nature, remaining within the droplets, and the reactive species in the continuous phase preferred to react with acrylic acid due to its significant concentration in cyclohexane. Meanwhile, the small portion of acrylic acid dissolved in the aqueous phase should not inhibit the polymerization in the particles. Interestingly, a plateau was observed again once acrylic acid was added, and no copolymer of acrylamide and acrylic acid was formed during the plateau period based on monitoring by GPC. This evidence further suggests that the radicals in the continuous cyclohexane phase (including radicals derived from initiator partitioned in the oil phase and reentry radicals from desorbed radicals) are the main source of nucleation of the particles in the RAFT inverse miniemulsion polymerization, which is consistent with the mechanism of Nomura et al.[54]

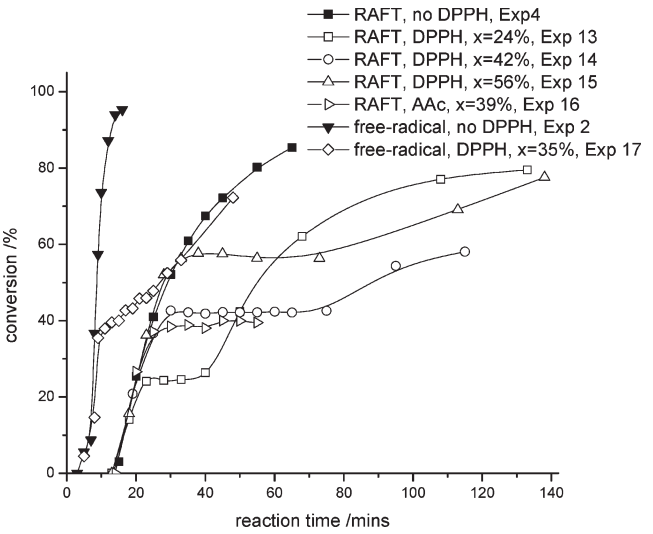

Figure 12. Effect of radical scavenger (DPPH and acrylic acid) on the RAFT and free-radical inverse miniemulsion polymerizations.

When DPPH was added to a free-radical inverse miniemulsion system, however, there is no such plateau (Exp17). Indeed, the polymerization continued, but at a slower rate than in the control (Exp2). This result suggests that a portion of the radicals was produced inside the particles and these nucleate the particles, which supports the theory of Asua et al.[55] At the same time, there was another fraction of radicals in the continuous phase that appeared to terminate due to reaction with DPPH, with these also contributing to the polymerization under normal circumstances (otherwise, there would be no retardation after the addition of DPPH).

Clearly, the particle nucleation process of inverse miniemulsion polymerization was influenced by the presence of the RAFT agent. The role of radicals inside the droplets was more pronounced in the nucleation process of the free-radical inverse miniemulsion polymerization, compared with the RAFT inverse miniemulsion polymerization. Such a different behavior between these two inverse miniemulsion polymerizations might be attributed to chain transfer reactions of initiator-derived radicals (including primary initiator radicals and reactive radicals that have added a few of monomer units) with RAFT agent within the particles. For free-radical inverse miniemulsion polymerizations, the newly born primary radicals from the initiator inside the particles will propagate by adding monomer units, terminate via radical recombination or with an incoming radical from the oil phase, or desorb from the particle into the continuous phase. For RAFT inverse miniemulsion polymerizations, other than the above fates, those initiator-derived radicals (primary initiator radicals and those after propagation) may suffer an additional chain transfer reaction with the RAFT agent. The propagating radicals may be lost either by desorbing into the continuous phase because of the short

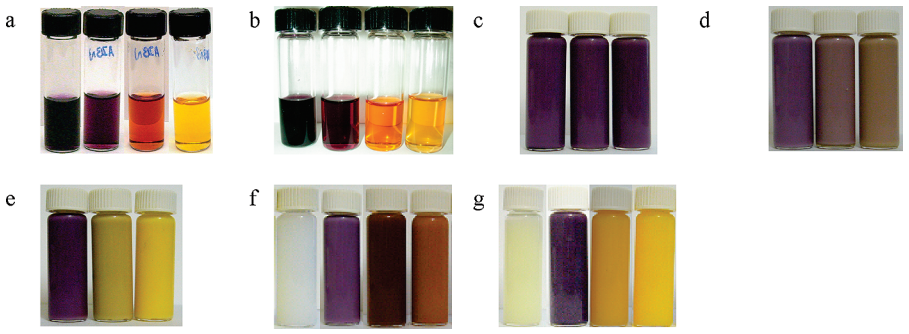

Figure 13. Evolution of color change of DPPH cyclohexane solution using different initiators. (a) AIBN, (b) BPO, and the evolution of color of inverse miniemulsions after the addition of DPPH at reaction time = 0 min. (c) Exp18, with only RAFT agent and AM in the aqueous phase. From left to right: t = 0, 50, 100 min. (d) Exp19, with only VA-044 in the aqueous phase. From left to right: t = 0, 50, 100 min. (e) Exp20, with only RAFT agent and VA-044 in the aqueous phase. From left to right: t = 0, 30, 40 min. (f) Exp21, free-radical inverse miniemulsion polymerization of AM. DPPH was added in the continuous phase at the beginning of the polymerization. From left to right: t = 0 (before adding DPPH), t = 0 (after adding DPPH), 30, 60 min. (g) Exp22, RAFT inverse miniemulsion polymerization of AM. DPPH was added in the continuous phase at the beginning of the polymerization. From left to right: t = 0 (before adding DPPH), t = 0 (after adding DPPH), 30, 40 min.

Table 3. Effects of Radical Scavengers on the Inverse Miniemulsion Polymerizations

Exp	monomer (M)	initiator (mM)	CTA (mM)	CTA/initiator	monomer/CTA	DPPH amount (mM)	acrylic acid (mM)	DPPH addition conv (%)
13	3.62	9.08	36.2	3.99	254	1.24		24
14	3.62	9.08	36.2	3.99	254	1.24		42
15	3.62	9.08	36.2	3.99	254	1.24		56
16	3.62	9.08	36.2	3.99	254		195	39
17	3.62	9.08				1.24		37
18	3.62		36.2		254	2.32		0
19		9.08				2.32		0
20		9.08	36.2	3.99		2.32		0
21	3.62	9.08				2.32		0
22	3.62	9.08	36.2	3.99	254	2.32		0

chain length or from transformation into RAFT intermediate radicals. Thus, the overall effect of the RAFT agent is to decrease the chance of propagating radicals in the particles for nucleation. Therefore, the influx of radicals within the particle for nucleation was lessened in RAFT inverse miniemulsion polymerizations compared with free-radical inverse miniemulsion polymerizations.

On the other hand, the difference of viscosity and diffusivity between free-radical and RAFT inverse miniemulsion polymerizations can also lead to a change in the population of propagating radicals in the particles. The average molecular weight of polymer is much higher in the free-radical inverse miniemulsion polymerization. The higher viscosity and lower diffusivity in the free-radical inverse miniemulsion polymerization can limit the mutual termination reaction of radicals in the particles. The higher survival probability of the propagating radicals inside the particles in free-radical inverse miniemulsion polymerization makes the difference in the nucleation process between the two systems more pronounced.

Exp18−Exp22 were designed to give further insight into the nucleation process of the free-radical and RAFT inverse miniemulsion polymerization. One advantage of using DPPH as radical scavenger is the significant color change with the consumption of DPPH.[59] Depending on the consumption of DPPH, the color of a DPPH solution can change significantly: from the original purple color to gray and brown. Then, once all the DPPH is consumed, it turns into an orange color. The color evolution of DPPH seems to be independent of the source of the radicals.[59,60] To further examine the correlation between the color of DPPH solution and DPPH consumption, AIBN and benzoyl peroxide (BPO) were dissolved in DPPH cyclohexane solution and heated to 70 °C to produce different radicals. As shown in Figure 13a,b, the color evolution of DPPH followed the same trend independent of the source of radicals. Therefore, the consumption rate of DPPH can be qualitatively assessed from the color change of DPPH. Figure 13 shows the color evolution of inverse miniemulsions with the addition of DPPH in the oil phase. Initially, all the inverse miniemulsions were purple in the presence of DPPH. Figure 13c shows that the miniemulsion in Exp18 remained purple after 100 min, suggesting that RAFT and acrylamide by themselves cannot generate radicals, as expected. For Exp19, VA-044 was added to the aqueous phase without RAFT agent and monomer, and in this case the miniemulsion color became brown (as shown in Figure 13d) after 100 min, suggesting no significant radical flux was produced into the continuous phase; i.e., there was significant geminate termination (two radicals generated in the particle were terminated pairwise) of VA-044 radicals in the particles.

From Figure 13c,d, no significant amount of desorbed radicals was generated when either RAFT agent or VA-044 was used separately. However, a combination of RAFT agent and VA-044 in Exp20 resulted in a fast color change of DPPH, as shown in Figure 13e, indicative of a significant flux of desorbed radicals into the continuous phase. Comparing Figure 13e with Figures 13c and 13d, it can be inferred that the initiator primary radicals can react with the RAFT agent and increase the radical desorption rate into the continuous phase, providing support for the above assumption of the chain transfer reaction of initiator-derived radicals with the RAFT agent resulting in the significantly different nucleation behavior of RAFT and free-radical inverse miniemulsion polymerizations. From Figure 13f,g, the radical desorption to the oil phase in free-radical inverse miniemulsion polymerization (Exp21) was significantly lower than in the RAFT inverse

miniemulsion polymerization (Exp22) since the RAFT inverse miniemulsion turned orange in a much shorter period while the brown color of Exp21 suggested there was certain amount of unreacted DPPH remaining. In addition, poly (acrylamide) was produced in Exp21, while no polymerization occurred in Exp22 until complete DPPH consumption after ~40 min, as indicated by the orange color of the miniemulsion at that time. Exp21 and Exp22 suggest that free-radical inverse miniemulsion polymerization has less radical desorption than RAFT inverse miniemulsion polymerization.

Fate of Desorbed Monomeric Radicals in Inverse Miniemulsion Polymerization. Steric surfactants can significantly change the kinetics of emulsion polymerizations and result in a barrier effect, i.e., a sharp decrease both in the exit and entry rate of oligomeric radicals.[49,58,61−65] As discussed above, the desorption of oligomeric radicals and RAFT induced radical loss can cause retardation of RAFT miniemulsion polymerizations,[39,40,66] and thus it is important to understand the fate of oligomeric radicals exiting to the continuous phase. Generally, these radicals can either reenter into the particle, propagate in the continuous phase to a critical degree, or suffer a termination with other radicals or dormant species in the continuous phase, as can be estimated by the following equations:[62−64]

For the entry rate of a monomeric radical R_{ads}:

$$R_{ads} = k_{ads}\frac{N_p}{V_{oil}N_{Av}}[R^\bullet] = 4\pi\frac{r_s(r_s+\delta)}{\delta + r_s D_h/D_{oil}} D_h \frac{N_p}{V_{oil}}[R^\bullet]$$

where k_{ads} is the absorption coefficient, N_p is the particle number, and N_{Av} is the Avogadro constant. r_s and δ are the average radius of particles and thickness of the surfactant hairy layer. D_h and D_{oil} are the diffusion coefficient of monomeric radicals in the surfactant layer and in oil phase. $[R^\bullet]$ is the concentration of monomeric radicals in the continuous phase. V_{oil} is the volume of the continuous phase.

The propagation rate of a monomeric radical R_p:

$$R_p = k_p[M]_{oil}[R^\bullet]$$

The termination rate of a monomeric radical R_t:

$$R_t = k_t[T^\bullet]_{oil}[R^\bullet]$$

For simplicity, the total radical concentration in the continuous phase $[T^\bullet]_{oil}$ can be estimated by

$$[T^\bullet]_{oil} \approx \sqrt{\frac{k_d f [I]_{oil}}{k_t}}$$

where k_p and k_t are the coefficient of propagation and termination reactions of a monomeric radical in the continuous phase. k_d is the decomposition coefficient of the initiator in the continuous phase.[67] $[M]_{oil}$ and $[I]_{oil}$ are the concentration of the monomer and the initiator partitioned in the oil phase, respectively. For a roughly estimation of $[T^\bullet]_{oil}$, the initiator efficiency factor f is assumed to be 1 considering the geminate termination of VA-044 in the oil phase can be trivial because of its low solubility in cyclohexane. Since trithiocarbonate has little chance of cross-termination of RAFT intermediate and propagating radicals and the RAFT agent used here has a very low solubility in the oil phase ($< 5 \times 10^{-6}$ mol/L), the effects of RAFT agent partitioned in the oil phase on the above rates are negligible.

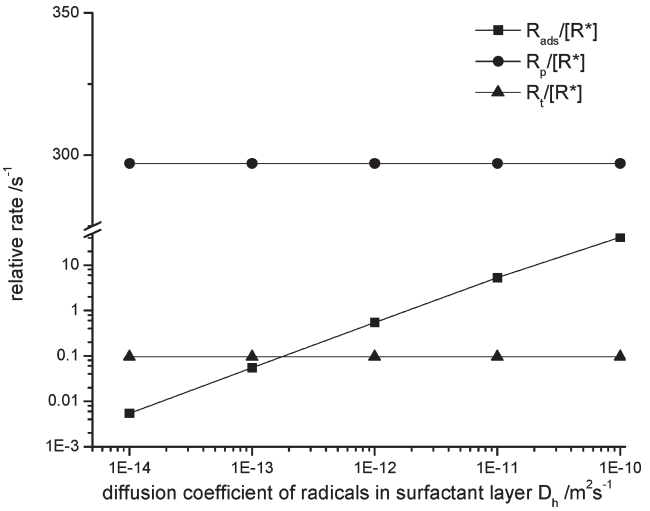

Figure 14. Relative rate of absorption, propagation, and termination reactions of monomeric radicals in the continuous phase.

Table 4. Parameter Values for the Evaluation of the Fate of Desorbed Monomeric Radicals[a]

parameter	value (units)	ref
r_s	105 nm	this work
δ	11 nm	47
D_{oil}	2.9×10^{-9} m^2/s	69
N_{Av}	6.0×10^{23} mol^{-1}	
N_p	2.0×10^{15} /L	this work
k_p	4.3×10^4 L mol^{-1} s^{-1}	42
k_d	1.4×10^{-4} s^{-1}	67
k_t	1.5×10^5 L mol^{-1} s^{-1}	42
$[I]_{oil}$	4.5×10^{-4} mol L^{-1}	this work
$[M]_{oil}$	0.0069 mol L^{-1}	this work
V_{oil}	51 mL	this work

[a] The dispersed phase of the inverse miniemulsion is pH = 4.

Figure 14 compares the relative values of the three rates with a variation of D_h and the related parameters listed in Table 4. The absorption rate decreases with a lower D_h while propagation and termination reactions remained constant. Unfortunately, the data of D_h (oil as continuous phase) are very limited in the literature. Considering that the D_h (water as continuous phase) usually has a value around 10^{-11}−10^{-12} m^2/s,[49,65] if D_h does not change much in the inverse system, then the most likely fate of monomeric radicals is to propagate in the continuous oil phase, as shown in Figure 14. The particle number and size were nearly constant during the RAFT inverse miniemulsion polymerizations. Therefore, it is suggested that the radicals of a critical chain length are captured by the particles, reenter into the particles, or are terminated inside or around the surfactant hairy layer instead of precipitating from the continuous phase and forming new particles. Since D_h decreases with an increase of chain length, the barrier effect of the steric surfactant would be more pronounced for these oligomeric radicals. As shown in Figure 14, the termination rate of the critical chain length radical is very close or even higher than the entry rate when $D_h < 1.1 \times 10^{-13}$ m^2 s^{-1}. Therefore, the fate of desorbed monomeric radicals could be propagation in the continuous phase to a critical degree followed by reentry into the particles. At the same time, a number of radicals may suffer a termination during the reentry step. The overall barrier effect on the monomeric radicals is to decrease significantly the reentry rate while boosting the termination rate.

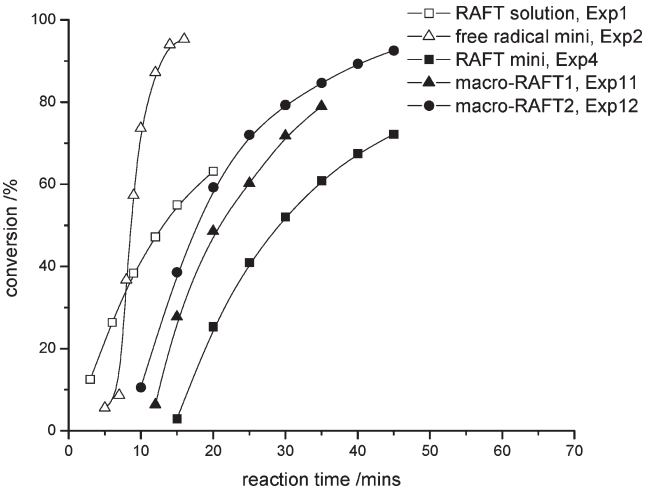

Figure 15. Comparison of induction times in RAFT inverse miniemulsion polymerizations with different RAFT agents, along with the RAFT solution polymerization and free-radical inverse miniemulsion polymerization.

From the above kinetic study, the mechanism of RAFT inverse miniemulsion polymerization of acrylamide using VA-044 as initiator is suggested as the following: most of VA-044 is partitioned in the dispersed aqueous phase. The radicals produced from this portion of VA-044 primarily suffer geminate termination via combination within the particles. The survived initiator-derived radicals (both initiator primary radicals and radicals after propagation) can undergo a chain transfer reaction with RAFT agent and generate the R group radical (acrylic acid group from the RAFT agent at the initial stage or oligomeric poly(acrylamide) group later on) that is likely to desorb through the hairy steric surfactant layer around the particles into the continuous oil phase. After propagation in the continuous oil phase, these desorbed radicals may terminate with other species in the oil phase to a large extent, since the reentry rate is reduced because of the larger chain length of these radicals. In addition to the VA-044 partitioned in the dispersed phase, a small fraction of VA-044 is dissolved in the oil phase. The primary initiator radicals produced in the oil phase can propagate to a critical chain length and irreversibly diffuse into the particle to initiate the polymerization, chain transfer to the RAFT agent, or terminate with other reactive species within the particles.

Figure 15 shows the induction times in the inverse miniemulsion polymerizations. Unlike benzyl dithioesters, trithiocarbonates usually do not result in a significant induction time for RAFT polymerizations since their RAFT intermediate radicals are less stable.[29,68] There was no induction time in the RAFT solution polymerization (Exp1). Compared with the free-radical inverse miniemulsion polymerization of Exp2, the RAFT inverse miniemulsion polymerization of Exp4 had a much longer induction time of ~15 min. The induction times of Exp11 and Exp12 using macro-RAFT agents tended to be shorter than when using monomeric RAFT agents (e.g., Exp4). The polymerization degree of the R group in macro-RAFT1 (Exp11) was about 5 while for macro-RAFT2 (Exp12) it was ~28. The shorter induction times in Exp11 and Exp12 indicate that the induction time can be affected by the chain length of the R group of RAFT agent. It was reported that the critical chain length of acrylamide in isooctane was 3.6.[42] Thus, there can be a significant loss of monomeric and oligomeric R group radicals of the RAFT agent. As mentioned above, after propagation in the continuous phase, these radicals can have a low reentry rate but a high termination rate. Therefore, the loss of oligomeric propagating radicals, among other potential reasons, may contribute to the induction time in the RAFT inverse miniemulsion polymerizations.

Conclusion

In this contribution, the kinetics of RAFT inverse miniemulsion polymerization were investigated in detail for the first time. The RAFT inverse miniemulsion polymerization of acrylamide exhibited typical behavior of controlled polymerizations when limited hydrolysis of the RAFT agent takes place. This behavior includes a linear relationship between M_n and the conversion, narrow PDI, and overlap of the RI and UV traces in the GPC curves. The effects of different reaction parameters on RAFT inverse miniemulsion polymerization were studied. Under the reaction conditions employed, a higher reaction temperature and a larger amount of the initiator increases the polymerization rate. When the aqueous phase is neutral or slightly acidic, the RAFT inverse miniemulsion polymerizations were better controlled compared with experiments at a pH above 7 (due to hydrolysis of the RAFT agent at high pH). An increase in the RAFT agent concentration tended to retard the polymerization and lower the average radical number per particle. The surfactant concentration had no effect on the polymerization rate and particle size.

The particle nucleation process in the inverse miniemulsion polymerizations was studied by the use of radical scavengers. In the RAFT inverse miniemulsion polymerizations, the radicals leading to particle nucleation mainly came from the continuous phase. In the free-radical inverse miniemulsion polymerizations, both radicals in the continuous phase and inside the particles contributed to the particle nucleation. The fate of desorbed monomeric radicals in inverse miniemulsion polymerizations was evaluated by the relative rates of propagation, reentry, and termination. One of the potential reasons for the induction time observed in the RAFT inverse miniemulsion polymerizations is suggested to be associated with desorption of oligomeric radicals below a critical chain length.

Acknowledgment. The authors thank the National Science Foundation (CTS-0553516) for funding this work and Uniqema for the supply of B246SF. C.W.J. thanks DuPont for a Young Professor Award and ChBE at GT for the J. Carl & Sheila Pirkle Faculty Fellowship.

References and Notes

(1) Wada, T.; Sekiya, H.; Machi, S. *J. Appl. Polym. Sci.* **1976**, *20* 3233–3240.
(2) Virk, P. S. *J. Fluid Mech.* **1971**, *45*, 225–46.
(3) Enright, D. P.; Perricone, A. C. *Petrol. Eng. Int.* **1988**, *60*, 55–56.
(4) Date, J. L.; Shute, J. M. *Tappi* **1959**, *42*, 824–826.
(5) Buck, S.; Pennefather, P. S.; Xue, H. Y.; Grant, J.; Cheng, Y.-L.; Allen, C. J. *Biomacromolecules* **2004**, *5*, 2230–2237.
(6) Lovell, P. A.; El Aasser, M. S. *Emulsion Polymerization and Emulsion Polymers*; Wiley: Chichester, 1997.
(7) Vanderhoff, J. W. *Polymerization and Polycondensation Processes*; American Chemical Society: Washington, DC, 1962.
(8) Landfester, K.; Willert, M.; Antonietti, M. *Macromolecules* **2000**, *33*, 2370–2376.
(9) Chou, Y. J.; El-Aasser, M. S.; Vanderhoff, J. W. *J. Dispersion Sci. Technol.* **1980**, *1*, 129–150.
(10) Qi, G. G.; Jones, C. W.; Schork, F. J. *Macromol. Rapid Commun.* **2007**, *28*, 1010–1016.
(11) Cunningham, M. F. *Prog. Polym. Sci.* **2008**, *33*, 365–398.
(12) Zetterlund, P. B.; Kagawa, Y.; Okubo, M. *Chem. Rev.* **2008**, *108*, 3747–3794.
(13) McLeary, J. B.; Klumperman, B. *Soft Matter* **2006**, *2*, 45–53.
(14) Pham, B. T. T.; Nguyen, D.; Ferguson, C. J.; Hawkett, B. S.; Serelis, A. K.; Such, C. H. *Macromolecules* **2003**, *36*, 8907–8909.

(15) Ferguson, C. J.; Hughes, R. J.; Nguyen, D.; Pham, B. T. T.; Gilbert, R. G.; Serelis, A. K.; Such, C. H.; Hawkett, B. S. *Macromolecules* **2005**, *38*, 2191–2204.
(16) Houillot, L.; Nicolas, J.; Save, M.; Charleux, B.; Li, Y. T.; Armes, S. P. *Langmuir* **2005**, *21*, 6726–6733.
(17) Manguian, M.; Save, M.; Chassenieux, C.; Charleux, B. *Colloid Polym. Sci.* **2005**, *284*, 142–150.
(18) van Zyl, A. J. P.; Bosch, R. F. P.; McLeary, J. B.; Sanderson, R. D.; Klumperman, B. *Polymer* **2005**, *46*, 3607–3615.
(19) Yang, L.; Luo, Y.; Li, B. *J. Polym. Sci., Polym. Chem.* **2006**, *44*, 2293–2306.
(20) Yang, L.; Luo, Y. W.; Li, B. G. *J. Polym. Sci., Polym. Chem.* **2005**, *43*, 4972–4979.
(21) Yang, L.; Luo, Y. W.; Li, B. G. *Polymer* **2006**, *47*, 751–762.
(22) Lu, F. J.; Luo, Y. W.; Li, B. G. *Macromol. Rapid Commun.* **2007**, *28*, 868–874.
(23) Luo, Y. W.; Gu, H. Y. *Polymer* **2007**, *48*, 3262–3272.
(24) Zhou, X. D.; Ni, P. H.; Yu, Z. Q. *Polymer* **2007**, *48*, 6262–6271.
(25) Bowes, A.; McLeary, J. B.; Sanderson, R. D. *J. Polym. Sci., Part A: Polym. Chem.* **2007**, *45*, 588–604.
(26) Ganeva, D. E.; Sprong, E.; de Bruyn, H.; Warr, G. G.; Such, C. H.; Hawkett, B. S. *Macromolecules* **2007**, *40*, 6181–6189.
(27) Klumperman, B. *Macromol. Chem. Phys.* **2006**, *207*, 861–863.
(28) Aston, M. S.; Herrington, T. M.; Tadros, T. F. *Colloids Surf.* **1989**, *40*, 49–61.
(29) Wang, R.; McCormick, C. L.; Lowe, A. B. *Macromolecules* **2005**, *38*, 9518–9525.
(30) Wu, C. *Handbook of Size Exclusion Chromatography and Related Techniques*; Marcel Dekker: New York, 2004.
(31) Albertin, L.; Stenzel, M.; Barner-Kowollik, C.; Foster, L.; Davis, T. *Macromolecules* **2004**, *37*, 7530–7537.
(32) One narrow distributed poly(acrylamide) GPC standard (M_w = 15 000, M_n = 12 800) was used to estimate the error due to the calibration method. The universal calibration method gives M_w = 18 357 and M_n = 14 081, an error about 22% higher than the true molecular weight of the GPC standard.
(33) Prescott, S. W.; Ballard, M. J.; Rizzardo, E.; Gilbert, R. G. *Macromolecules* **2002**, *35*, 5417–5425.
(34) Thomas, D. B.; Convertine, A. J.; Hester, R. D.; Lowe, A. B.; McCormick, C. L. *Macromolecules* **2004**, *37*, 1735–1741.
(35) Thomas, D. B.; Convertine, A. J.; Myrick, L. J.; Scales, C. W.; Smith, A. E.; Lowe, A. B.; Vasilieva, Y. A.; Ayres, N.; McCormick, C. L. *Macromolecules* **2004**, *37*, 8941–8950.
(36) Albertin, L.; Stenzel, M. H.; Barner-Kowollik, C.; Davis, T. P. *Polymer* **2006**, *47*, 1011–1019.
(37) Mertoglu, M.; Laschewsky, A.; Skrabania, K.; Wieland, C. *Macromolecules* **2005**, *38*, 3601–3614.
(38) Baussard, J.; Habib-Jiwan, J.; Laschewsky, A.; Mertoglu, M.; Storsberg, J. *Polymer* **2004**, *45*, 3615–3626.
(39) Monteiro, M. J.; Hodgson, M.; De Brouwer, H. *J. Polym. Sci., Part A: Polym. Chem.* **2000**, *38*, 3864–3874.
(40) Prescott, S. W.; Ballard, M. J.; Rizzardo, E.; Gilbert, R. G. *Macromolecules* **2005**, *38*, 4901–4912.
(41) Kwak, Y.; Goto, A.; Tsujii, Y.; Murata, Y.; Komatsu, K.; Fukuda, T. *Macromolecules* **2002**, *35*, 3026–3029.
(42) Platkowski, K.; Pross, A.; Reichert, K. H. *Polym. Int.* **1998**, *45*, 229–238.
(43) Seabrook, S. A.; Tonge, M. P.; Gilbert, R. G. *J. Polym. Sci., Part A: Polym. Chem.* **2005**, *43*, 1357–1368.
(44) Luo, Y.; Wang, R.; Yang, L.; Yu, B.; Li, B.; Zhu, S. *Macromolecules* **2006**, *39*, 1328–1337.
(45) Qi, G.; Schork, F. J. *Langmuir* **2006**, *22*, 9075–9078.
(46) Kobyakova, K. O.; Gromov, V. F.; Teleshov, E. N. *Polym. Sci.* **1993**, *35*, 151–155.
(47) HernandezBarajas, J.; Hunkeler, D. J. *Polymer* **1997**, *38*, 437–447.
(48) Hunkeler, D.; Hamielec, A. E.; Baade, W. *Polymer* **1989**, *30*, 127–142.
(49) Thickett, S. C.; Gilbert, R. D. *Macromolecules* **2007**, *40*, 4710–4720.
(50) Maxwell, I. A.; Morrison, B. R.; Napper, D. H.; Gilbert, R. G. *Macromolecules* **1991**, *24*, 1629–1640.
(51) Casey, B. S.; Morrison, B. R.; Maxwell, I. A.; Gilbert, R. G.; Napper, D. H. *J. Polym. Sci., Part A: Polym. Chem.* **1994**, *32*, 605–630.
(52) Schork, F.; Luo, Y.; Smulders, W.; Russum, J.; Butte, A.; Fontenot, K. *Polym. Particles* **2005**, *175*, 129–255.
(53) Alshahib, W. A. G.; Dunn, A. S. *Polymer* **1980**, *21*, 429–431.
(54) Nomura, M.; Fujita, K. *Makromol. Chem. Rapid* **1989**, *10*, 581–587.
(55) Asua, J.; Rodriguez, V.; Sudol, E.; Elaasser, M. *J. Polym. Sci., Part A: Polym. Chem.* **1989**, *27*, 3569–3587.
(56) Luo, Y.; Schork, F. *J. Polym. Sci., Part A: Polym. Chem.* **2002**, *40*, 3200–3211.
(57) Nomura, M.; Suzuki, K. *Ind. Eng. Chem. Res.* **2005**, *44*, 2561–2567.
(58) Autran, C.; de la Cal, J. C.; Asua, J. M. *Macromolecules* **2007**, *40*, 6233–6238.
(59) Espin, J. C.; Soler-Rivas, C.; Wichers, H. J. *J. Agric. Food Chem.* **2000**, *48*, 648–656.
(60) Schwarz, K.; Bertelsen, G.; Nissen, L. R.; Gardner, P. T.; Heinonen, M. I.; Hopia, A.; Huynh-Ba, T.; Lambelet, P.; McPhail, D.; Skibsted, L. H.; Tijburg, L. *Eur. Food Res. Technol.* **2001**, *212*, 319–328.
(61) Baade, W.; Reichert, K. H. *Eur. Polym. J.* **1984**, *20*, 505–512.
(62) Gilbert, R. G. *Emulsion Polymerization: A Mechanistic Approach*; Academic: London, 1995.
(63) Thickett, S. C.; Gilbert, R. G. *Macromolecules* **2006**, *39*, 2081–2091.
(64) Thickett, S. C.; Gilbert, R. G. *Macromolecules* **2006**, *39*, 6495–6504.
(65) Asua, J. M. *Macromolecules* **2003**, *36*, 6245–6251.
(66) Butte, A.; Storti, G.; Morbidelli, M. *Macromolecules* **2001**, *34*, 5885–5896.
(67) The decomposition coefficient of VA-044 at 60 °C is estimated based on the data provided by the manufacturer: The activation energy of VA-044 $E_a = 1.08 \times 10^5$ J/mol and the decomposition cofficient $k_d = 1.15 \times 10^{-3}$ min^{-1} at 44 °C.
(68) Chong, Y.; Krstina, J.; Le, T.; Moad, G.; Postma, A.; Rizzardo, E.; Thang, S. *Macromolecules* **2003**, *36*, 2256–2272.
(69) Capek, I. *Des. Monomers Polym.* **2003**, *6*, 399–409.